Fluid-induced organic synthesis in the solar nebula recorded in extraterrestrial dust from meteorites

Christian Vollmer[a,1], Demie Kepaptsoglou[b], Jan Leitner[c], Henner Busemann[d], Nicole H. Spring[d], Quentin M. Ramasse[b], Peter Hoppe[c], and Larry R. Nittler[e]

[a]Institut für Mineralogie, Universität Münster, D-48149 Münster, Germany; [b]SuperSTEM Laboratory, Science & Technology Facilities Council Daresbury Laboratories, Daresbury WA4 4AD, United Kingdom; [c]Abteilung Partikelchemie, Max-Planck-Institut für Chemie, D-55128 Mainz, Germany; [d]School of Earth, Atmospheric and Environmental Sciences, University of Manchester, Manchester M13 9PL, United Kingdom; and [e]Department of Terrestrial Magnetism, Carnegie Institution of Washington, NW, Washington, DC 20015

Edited by Mark H. Thiemens, University of California, San Diego, La Jolla, CA, and approved September 15, 2014 (received for review May 4, 2014)

Isotopically anomalous carbonaceous grains in extraterrestrial samples represent the most pristine organics that were delivered to the early Earth. Here we report on gentle aberration-corrected scanning transmission electron microscopy investigations of eight ^{15}N-rich or D-rich organic grains within two carbonaceous Renazzo-type (CR) chondrites and two interplanetary dust particles (IDPs) originating from comets. Organic matter in the IDP samples is less aromatic than that in the CR chondrites, and its functional group chemistry is mainly characterized by C–O bonding and aliphatic C. Organic grains in CR chondrites are associated with carbonates and elemental Ca, which originate either from aqueous fluids or possibly an indigenous organic source. One distinct grain from the CR chondrite NWA 852 exhibits a rim structure only visible in chemical maps. The outer part is nanoglobular in shape, highly aromatic, and enriched in anomalous nitrogen. Functional group chemistry of the inner part is similar to spectra from IDP organic grains and less aromatic with nitrogen below the detection limit. The boundary between these two areas is very sharp. The direct association of both IDP-like organic matter with dominant C–O bonding environments and nanoglobular organics with dominant aromatic and C–N functionality within one unique grain provides for the first time to our knowledge strong evidence for organic synthesis in the early solar system activated by an anomalous nitrogen-containing parent body fluid.

solar nebula | organic matter | meteorites | comets | transmission electron microscopy

Primitive extraterrestrial materials, including unmetamorphosed carbonaceous chondrites, chondritic porous interplanetary dust particles (CP-IDPs), carbonaceous Antarctic micrometeorites, and material from comet 81P/Wild 2, contain isotopically anomalous carbonaceous matter typically enriched in D and/or ^{15}N compared with the Earth and bulk meteorites (1–11). This carbonaceous matter occurs as diffuse material but also in the form of sub-μm– to μm-sized grains that are extremely enriched in D and/or ^{15}N and therefore stand out in isotopic maps as so-called "hot spots." These hot spots represent good candidates to study ancient organic compounds that may have served as precursors for the prebiotic history of the early Earth. In many, but not all, cases, the isotopic hot spots occur as so-called "nanoglobules," which are observed as hollow or compact carbonaceous sub-μm spheres in a wide range of primitive extraterrestrial samples (e.g., refs. 11–16). The most widely accepted theory for the origins of the anomalies invokes exothermic ion–molecule isotope exchange reactions at very low temperatures (<25 K) in cold interstellar clouds or the outer reaches of the nascent solar nebula (e.g., refs. 6, 7, 17, and 18). A second possible mechanism for the observed ^{15}N enrichments is N_2 self-shielding, in which optical depth effects lead to isotope-selective photodissociation (19–22), but the applicability of the N_2 self-shielding model to the observed ^{15}N anomalies is still uncertain.

Correlated isotopic and structural information on these organic grains is sparse. Secondary ion mass spectrometry (SIMS) at high spatial resolution [~100 nm can be achieved by Cameca NanoSIMS instruments (23)] in combination with transmission electron microscopy (TEM) allows the analysis of both isotopic composition and electronic bonding configuration on a sub-μm scale. These investigations are important to understand the origins and evolution of complex organic compounds in ancient meteoritic materials that contributed to the organic inventory of early Earth. Such combined studies have so far been performed, e.g., on organic grains in the Tagish Lake meteorite (15, 24), IDPs (5, 13, 25), comet 81P/Wild 2 material (9, 10), insoluble organic matter (IOM) extracted from meteorites (11, 26), and matrix regions in Renazzo-type (CR) and Ivuna-type (CI) chondrites (27–29) all applying only standard TEM techniques. Recently, synchrotron X-ray absorption near-edge structure (XANES) analyses have been performed on these organic grains before further TEM investigations (e.g., refs. 10, 11, 26, and 30). These analyses can reveal the bonding configuration of organic grains with high energy resolution (~0.1 eV) and relatively high spatial resolution (~20 nm) (9).

Functionality studies of IOM, IDPs, and comet 81P/Wild 2 material (e.g., refs. 2, 3, 5, 9–13, 16, 25, 26, 30, and 31) as well as combined isotope functionality studies (5, 11, 24, 26, 32) show that meteoritic IOM as well as cometary organics from IDPs and Wild 2 are relatively similar in their dominant functional group characteristics. The meteoritic IOM component can be quite complex but is in general characterized by three main bonding environments, i.e., aromatic C=C, aromatic ketone or aldehyde bonding, and carboxyl bonding (Table S1) (ref. 9 and references therein). The two latter bands can be assigned to the existence of

Significance

Organic matter from the parent molecular cloud of our solar system can be located in primitive extraterrestrial samples like meteorites and cometary grains. This pristine matter contains among the most primitive organic molecules that were delivered to the early Earth 4.5 billion years ago. We have analyzed these organics by a high-resolution electron microscope that is exceptionally suited to study these beam-sensitive materials. Different carbon and nitrogen functional groups were identified on a submicron scale and can be attributed to early cometary and meteoritic organic reservoirs. Our results demonstrate for the first time to our knowledge that certain highly aromatic and nitrogen-containing ubiquitous organics were transformed from an oxygen-rich organic reservoir by parent body fluid synthesis in the early solar system.

Author contributions: C.V., J.L., and H.B. designed research; C.V., D.K., J.L., H.B., N.H.S., and Q.M.R. performed research; C.V., D.K., J.L., H.B., N.H.S., Q.M.R., P.H., and L.R.N. analyzed data; and C.V. wrote the paper.

The authors declare no conflict of interest.

This article is a PNAS Direct Submission.

[1]To whom correspondence should be addressed. Email: christian.vollmer@wwu.de.

This article contains supporting information online at www.pnas.org/lookup/suppl/doi:10.1073/pnas.1408206111/-/DCSupplemental.

C–O bonding environments. The IOM-like functionality represents a common reservoir from which other, chemically more complex or more polymerized organic compounds may have evolved. Models on the molecular structure of IOM from the CM carbonaceous chondrite Murchison agree well with this overall functional group chemistry, where small aromatic units are interconnected by aliphatic, oxygenated, and N-containing chains (33). A further component has been identified among organic grains, usually best preserved in nanoglobules (11, 12, 15, 16). The organic functionality of nanoglobules is in general also IOM-like but often more aromatic with stronger absorption at 285 eV. Some nanoglobules may derive from circumstellar settings as highly primitive polycyclic aromatic hydrocarbons (PAHs) (34) or form late on the parent bodies by aqueous alteration reactions. Cody et al. (35) have recently suggested that the bulk of IOM found in chondrites can be synthesized from soluble formaldehyde (H_2CO) moieties which evolve into more complex, aromatic units upon progressive polymerization by aqueous alteration on the parent body. This model was further supported by experimental work (36), but the role of anomalous nitrogen in these fluid scenarios has not been demonstrated yet on true samples. Furthermore, the resulting evolution of pristine organic matter with respect to electronic bonding configuration and chemical constitution in these synthesis models is still poorly constrained.

We present here an alternative way to investigate these organic grains with superior spatial resolution, via the Nion UltraSTEM 100 analytical aberration-corrected scanning TEM (STEM) operated at a low acceleration voltage of 60 kV. The flexibility offered by this type of microscope is ideal for investigating organic grains. The instrument can be operated in so-called "gentle STEM" conditions (37) below the knock-on damage threshold for carbon [<~80kV (38)], while retaining a much higher spatial resolution than X-ray techniques. Moreover, the probe current and electron dose can be tailored to minimize ionization damage (39). The microscope operates with a cold field emission electron source achieving an energy spread of only ~0.3 eV without a monochromator. This energy resolution is only marginally worse than synchrotron XANES while still maintaining a very high spatial resolution (~0.1 nm at 60 kV). We used the UltraSTEM to observe and analyze eight isotopically anomalous organic grains identified by NanoSIMS ion imaging within four different primitive extraterrestrial samples: two CR2 chondrites, Northwest Africa (NWA) 852 and the Antarctic Graves Nunataks (GRA) 95229, and two IDPs. Both IDPs in this study are from the L2036 collector (cluster 20, AK 5 and 6, IDP AK5, and IDP AK6) (Table S2 and *Materials and Methods*). The STEM data provide combined morphological and structural details of isotopically anomalous organic grains with electronic bonding configuration analyses by electron energy loss spectroscopy (EELS). Our results provide the first direct observational evidence to our knowledge for an alteration scenario of anomalous organics on the CR parent body and how the two organic components described above can be linked by transformation reactions.

Results

The two ^{15}N-rich grains from NWA 852 (2_24a and 2_24b) are relatively large (>500 nm), compact, and elliptical and stand out in STEM images by their smooth contrast (Fig. 1 *A* and *B* and Table S2). The grains share similar morphological characteristics and also have similar isotopic compositions within three SDs, so they are most probably genetically connected. They are also located right next to large cracks visible in the SEM (Fig. S1). The ^{15}N-rich grain 13_4 from GRA 95229 has a roundish, globular morphology with a hollow center; the GRA 95229 ^{15}N-rich grain 14_2 appears compact and has an irregular, slightly roundish shape (Fig. S2). The IDP grains are generally smaller than the ones targeted in the CR chondrites making it difficult to relocate grains for focused ion beam (FIB) preparation (Figs. S3 and S4).

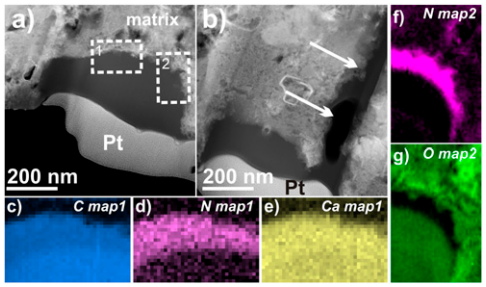

Fig. 1. UltraSTEM images and EELS chemical maps of organic grains from NWA 852. (*A*) Overview HAADF image of grain 2_24a with the area of the two EELS maps outlined by white boxes. The grain has homogeneous and dark contrast. (*B*) Overview HAADF image of grain 2_24b. A lobe of organic material extends into the surrounding matrix (marked by arrows). (*C*–*G*) EELS chemical maps in the areas outlined in *A* with the enrichment of nitrogen in the rim part of the grain, the Ca enrichment, and opposite distribution of nitrogen and oxygen clearly visible.

The grains 2_24a+b from NWA 852 are amorphous and show no signs of crystalline inclusions, neither in bright field (BF) nor in high-angle annular dark field (HAADF) imaging modes (Fig. 1 *A* and *B*). No graphene sheets (i.e., lattice planes indicative of graphite crystallization with $d_{0002} = 0.34$ nm) nor development of serpentine-like phases could be observed within these distinctively homogeneous grains in high-resolution (HR) STEM images across different regions. The potential presence of graphitic sheets would indicate thermal overprint (31), whereas serpentine-like minerals would give a hint for aqueous alteration. However, the organic grain was apparently distributed into the matrix because a lobe of the grain extends farther down the section from grain 2_24b (Fig. 1*B*).

Contrary to the uniformity suggested by the image contrast of grain 2_24a, EELS reveals a chemical heterogeneity and changes in its electronic bonding configuration (Figs. 1 *C*–*G* and 2). In addition to C, the grain also contains Ca and N, as evidenced by the presence of C–K, Ca–$L_{2,3}$, N–K, and O–K edges in the EEL spectra (Fig. 2 *A*–*D*). EELS elemental mapping (Figs. 1*D* and 2*A*) shows that N is heterogeneously distributed throughout the grain and concentrates mainly within a ~50–100 nm thin rim encasing the grain. Oxygen on the other hand shows the opposite trend and is rather depleted in that rim (Figs. 1*G* and 2*D*). The N–K edge in this rim could be recorded successfully with high signal-to-noise ratio (Fig. 2*C*) without any damage observed in subsequent imaging. The edge shows a broad (~3 eV width) π^* peak at ~398.8 eV attributed to imine (double) or nitrile (triple) C–N bonding and further bands above 400 eV explainable by N heterocycles (Table S2) (e.g., ref. 9 and EELS references therein and refs. 26 and 30). It is noted that small energy shifts between this and previous work on nitrile functionality (9, 26) should be expected due to small differences in calibration and slightly lower energy resolution of the EELS measurements. From the EEL spectra it was also possible to obtain relative elemental abundances by quantification of combined C–K and N–K edges by standard EELS quantification routines. The calculated atomic N/C ratio from a cumulative EEL spectrum of this rim is 0.14 ± 0.02. Another significant difference between the rim and interior of the grain is found in the fine structure of the C–K edge acquired within the two areas (Fig. 2*A*). Whereas the rim displays the dominant feature at ~285.1 eV of aromatic C, this band is less pronounced in the core and instead shows two smaller peaks ~1 eV apart at ~285.1 and ~286.5 eV (Table S2). The interior has a distinct extra shoulder at ~283 eV, which can be explained by C=O bonding environments (40). The second feature at ~286.5 eV can as well be attributed to functional groups involving oxygen bonding, i.e., aldehyde (286.3 eV) or ketone (286.6–286.8 eV) as

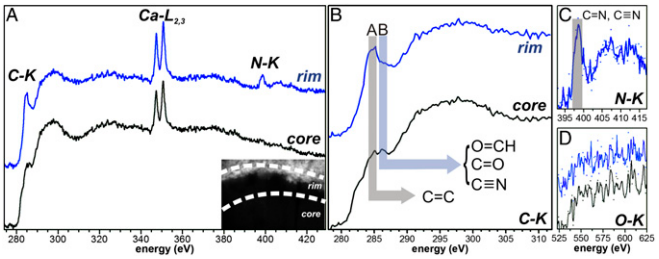

Fig. 2. EEL spectra at the different absorption edges of the N-rich rim and the core of organic grain 2_24a from NWA 852 (inset HAADF image) with the most prominent edges marked (Table S2). (*A*) The two white lines around 350 eV are due to Ca, but a distinct carbonate band around 290 eV is not recognizable. The N–K edge is not visible anymore in the spectrum of the core of the grain. (*B–D*) Close-up view of EEL spectra at the C–K, N–K, and O–K edges with the most prominent bands marked by vertical lines in *B*. The aromatic feature at around 285 eV is clearly diminished in the core, which instead shows an additional band at around 286 eV attributable to C–O bonding environments. The distinct N–K edge shows a strong band at around 399 eV indicative of imine and nitrile functionality but also some hint for N-heterocycles (Table S2).

well as nitrile C≡N triple bonding (Table S2) (9). No peak centered at ∼291.7 eV could be identified, which would have indicated the development of graphene sheets due to thermal metamorphism (41), which is in accordance with the absence of graphitic fringes in HR images. Dominant so-called "white" lines of Ca (Ca–$L_{2,3}$ edge) are also present in the spectra throughout both grains in NWA 852 with no difference between the rim and the interior of grain 2_24a (Figs. 1*E* and 2*A*). The Ca–$L_{2,3}$ edge is also visible in the lobe that extends into the FIB section. The Ca content is not associated with any crystalline grains nor is a sharp σ* C–K edge peak observed at 290.3 eV that would have been indicative of carbonate bonding (refs. 5 and 24 and references therein). Also, the matrix in the direct vicinity of the organic grains does not contain any detectable Ca (Fig. 1*E*).

HAADF images of grain 13_4 from GRA 95229 (Fig. 3*A*) show a patchy and heterogeneous contrast apparently originating from small particles dispersed within the carbonaceous material. HR imaging reveals the presence of tiny calcite crystals only several nm in size that add discrete contrast to the images (Fig. S2). EELS in this area of the grain shows dominant bands at ∼284.8 eV (aromatic C), at ∼286.5 eV (aldehyde/ketone or nitrile bonding), and at ∼290 eV, which can be attributed to carbonate bonding. The calcium white lines are also detected at ∼346 eV, which underlines the presence of calcite crystals. The N–K edge is not as dominant as in the NWA 852 grains but still resolvable above the background with a broad band at ∼399 eV (Fig. 3*C*). However, upon further analysis, the N–K edge degraded quickly and was not as stable as in the NWA 852 grains. The grain 14_2 is homogeneous in HAADF imaging (Fig. 3*B*) and does not display any crystallinity in the images. EEL spectra over this homogeneous part of the grain exhibit characteristic π* bands attributed to aromatic C and C–O bonding as well as the σ* transition bands with an imposed carbonate band at ∼290 eV and again small Ca peaks. A distinct N–K edge could not be detected in this area.

The IDP organic grains appear irregular (Fig. 4 *A–D*) and are intermixed and surrounded by silicates and sulfides. For example, grain 08 from IDP AK5 is elongated and fills the gap between a large Fe sulfide visible to the right and a hole filled with Pt to the left (Fig. 4*A*). This supports the view that IDP organics often glue more refractory materials together rather than being encompassed in discrete grains (42). Some internal crystallites are visible in BF and HAADF images (Fig. 4 *A–D*), but these are exclusively Au and Pt nanoparticles redeposited from the FIB preparation and are distinguishable by their high Z contrast in HAADF imaging. The organic grains from the IDPs analyzed here exhibit a smooth, i.e., chemically and structurally homogeneous, contrast. HR imaging reveals that the grains are amorphous and show no signs of internal short- or long-range order within different areas. No graphitization could be observed and no crystalline inclusions are encompassed within the organic grains, with the exception of the aforementioned Au and Pt nanoparticles. It was possible to acquire EEL spectra on relatively clean regions of the grains without significant contribution from Au and/or Pt. All IDP organic grains exhibit a similar pattern in general: the π* antibonding transition is greatly diminished compared with the large σ* transition, but small bands within the flank of the main C–K edge can still be resolved at 284.7 eV (aromatic C), around 286 eV (ketone/aldehyde bonding), and around 287 eV (aliphatic C) (Table S1 and Fig. 4). A noisy and not well-resolved N–K edge is observed in spectra from grain 11 at ∼399 eV (Fig. S5). No electron energy loss at the N–K edge could be observed in the other IDP organic grains. Small Ca–$L_{2,3}$ peaks are visible in grains 8 and 11 (Fig. S5).

Discussion

Organic grains in the solar nebula were prone to asteroidal and terrestrial alteration reactions. Asteroidal alteration was active to varying degrees even within the same meteorite parent body on a decimeter scale. For example, in the Tagish Lake carbonaceous chondrite (43), there is a decreasing abundance of aromatic carbon compounds with high D/H ratios in bulk organic matter from different parts of this meteorite, and these variations are strongly correlated with independent mineralogical measures of aqueous alteration (44). Thus, comparison of organic characteristics in different materials with different alteration histories allows an improved understanding of the nature of unaltered molecular cloud material and the effects of later transformation reactions, e.g., on the parent bodies. It is possible that diverse functionality of organic grains has been inherited from the interstellar medium or that the main transformation reactions occurred in the solar nebula or even later on respective parent bodies (e.g., refs. 45 and 46). It is therefore crucial to distinguish these contrasting transformation scenarios by direct functionality analyses on anomalous organic grains from different parent bodies, e.g., asteroids and comets.

It has been shown that the ratio of aliphatic to aromatic functional groups is higher in organic matter from IDPs than in that from meteorites (25). This can be explained by less

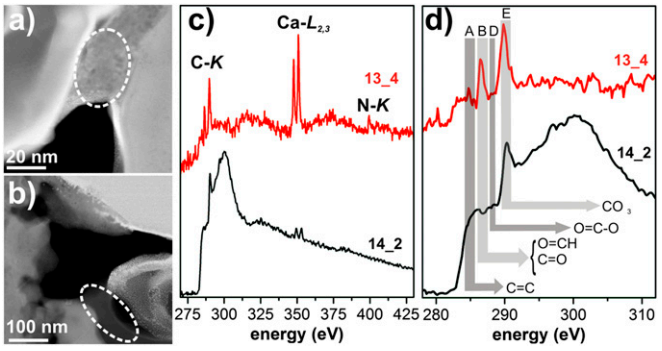

Fig. 3. UltraSTEM images and EEL spectra of grains 13_4 and 14_2 from GRA 95229. (*A*) HAADF overview image of the remaining material of grain 13_4 (encircled) with distinct mottled contrast due to crystalline inclusions. (*B*) HAADF overview image of the remaining material of grain 14_2 (encircled) with clean and homogeneous contrast. (*C* and *D*) Extracted EEL spectra from the grains with distinct bands around the carbon K edges marked. White lines of Ca are again visible at ∼346 eV in both grains and at ∼290 eV due to carbonate bonding. The N–K edge is rather noisy in grain 13_4 but clearly resolvable above the background.

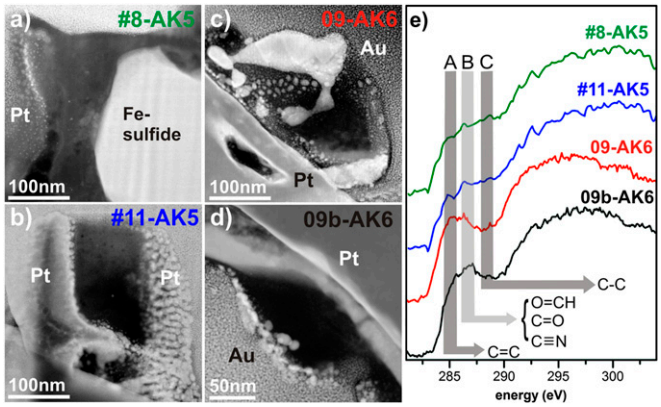

Fig. 4. UltraSTEM images and corresponding EEL spectra of grains from both studied IDPs. (*A*) HAADF image of the irregular grain 8 from IDP AK5, which is enclosed by a large Fe sulfide to the right and Pt to the left. (*B*) HAADF image of the blocky grain 11 from IDP AK5 enclosed by Au and Pt from the substrate and preparation, respectively. (*C*) HAADF image of the irregular organic grain 09 from IDP AK6 with higher Z-contrast material (Pt from FIB preparation and/or Au from the substrate) penetrating the grain. (*D*) HAADF image of the grain 09b from IDP AK6 sandwiched between the Pt cover (upper right) and the Au substrate (lower left) as well as diverse silicates in the direct vicinity. (*E*) Extracted stacked EEL spectra of all IDP grains with distinct bands around the C–K edge again marked (Table S2). The two characteristic IOM-like bonding environments at ~285 eV and ~286 eV are clearly visible in all spectra, together with a small peak at ~287 eV.

modification of IDP organics relative to meteoritic IOM because modification of carbonaceous matter destroys the more labile aliphatic bonding compared with aromatic domains. This could also be shown in various lithologies of the Tagish Lake meteorite, where a decreasing H/C ratio (a proxy for the length of aliphatic carbon chains) decreases with increasing aromaticity and alteration degree (43). The more aliphatic functionality of more primitive IDP organics can be observed in the present work by the observation of absorption bands at ~287 eV (Fig. 4*E*). The organic grains observed by Keller et al. (25) and in this work therefore support the view that more pristine organic matter can be defined by higher aliphatic to aromatic ratios and a higher level of C–O bonding of respective carbonaceous material. Mineralogical observations have demonstrated that in contrast to IDPs, fluids in CR and other carbonaceous chondrites have redistributed isotopically anomalous organics and that these carbonaceous materials often occur in veins and fine networks within chondrite matrices and not always as compact, distinct grains (32). However, the effect of this fluid redistribution on organic functional group chemistry is still not well understood. The functionality of organic grains from NWA 852 and GRA 95229 compared with the IDP organics in this study can give important insights into these complex evolutionary models and the role of fluids. It is important to note here that this pristine starting material with abundant C–O bonding environments found in IDPs must not necessarily be isotopically anomalous.

The UltraSTEM investigations on grains 2_24a+b are crucial in this respect, especially because grain 2_24a encompasses the formation and alteration pathways described above within a very limited area. The internal chemical and functional group heterogeneity can lend support to the following modification mechanisms being possibly active within grain 2_24a: (*i*) the grain formed by thermal metamorphism of an initial C–H–O–N–rich organic matter by loss of H and N in the interior, which led to the formation of the N-rich rim, whereas O is retained (31, 45). However, such a thermal overprint would need high temperatures at long duration times (31), and these conditions can be ruled out on the CR chondrite parent body, whose meteorites are usually of petrologic type 2. We therefore conclude that the observed rim texture of grain 2_24a is not due to thermal metamorphism of organic matter. (*ii*) The texture and heterogeneous N distribution may represent a FIB preparation artifact. However, in that case we would expect to see not a rim but a gradient with a boundary parallel to the original surface. Also, in other grains prepared by the FIB technique, such a dramatic effect on chemical functionality has not been observed. (*iii*) The more aromatic rim of the grain may have formed by complex UV irradiation and warming reactions of a more pristine precursor in the solar nebula (47). UV irradiation leads to breakup of organics into more reactive ions and radicals, which can then reorganize, maybe in a fluid or in the nebula, to eventually form more complex organic molecules seen in meteorites. The problem with this model with respect to our grain is that even if N was present in that grain as some ice mantle before UV irradiation, it is not plausible why this irradiation would aromatize the grain to the exact depth of the previous N-rich mantle. Aromatization and N content would more likely be decoupled in that case, which is not observed. We therefore rule out this possibility. (*iv*) N-rich organic matter with a high abundance of polyaromatic domains as observed (Fig. 2*B*) may form through formose reactions in a fluid on the parent body as proposed by Cody et al. (35). This model requires temperatures around 50 °C to polymerize the small formaldehyde molecules, which is well conceivable locally on meteorite parent bodies (48). However, it is questionable whether meteorite parent bodies contained excess formaldehyde, but it is still possible that other, simple organic compounds with C–O bonding environments (ketone/aldehyde) served as precursor organic material for hydrous reactions to occur. A fluid transporting anomalous ^{15}N-rich soluble molecules must then have reacted with this precursor material, as evidenced by the sharp reaction front between the interior and rim of the grain in STEM-EELS chemical maps (Fig. 1 *C*–*G*). Redistribution reactions of N-rich organics that do not erase isotopic anomalies have been observed, albeit rarely in other work (e.g., ref. 27). In organic matter from comet Wild 2, Cody et al. (30) have noticed heterogeneously distributed N in one area of one grain. We therefore favor an organic synthesis model that involves a ^{15}N-containing fluid on the meteorite parent body (35) that reacted with a more pristine organic matter containing abundant ketone/aldehyde functionality. We believe the striking rim-like texture we report in grain 2_24a is the first direct evidence to our knowledge that anomalous nitrogen can be transported in a fluid and transform single organic grains, which must not necessarily have been anomalous themselves.

We additionally observe very pronounced N functionality. The strongest N–K edge features appear around 399 eV in the CR chondrite organic grains, most likely due to C–N double (imine) and triple (nitrile) bonding environments (9, 26), but there is also evidence for the presence of N heterocycles such as pyrrole or imidazole having absorption above 400 eV (11, 49) (Table S1). C–N double and triple bonding is consistent with isotopic fractionation models involving HCN molecules (50), but it is well known that these organic molecules are prone to hydrous parent body redistribution reactions that do not erase isotopic anomalies (e.g., ref. 51). Therefore, the molecular cloud organics carrying isotopic anomalies from fractionation reactions have been dissolved in a fluid retaining their anomalies but have also been transformed into other, more soluble organics such as ammonia known to be present in meteorite parent bodies (52). Experimental work has demonstrated that ammonia in the fluid increases the polymerization rate in formose reactions and leads to substantial incorporation of nitrogen into organic matter (36), which supports our observation. These hydrous reactions also more likely form N heterocycles such as pyrrole or imidazole, which is consistent with observed N functionality. These N heterocycles were also detected in Murchison IOM and are suggested to be present based on models of IOM molecular structure (33). We

therefore see a mixture of the original imine/nitrile functionality from isotopic fractionation and N heterocycles from hydrous polymerization reactions. The lack of strong N functional group chemistry in the IDP organics is more difficult to explain. Given the microscale diversity of IDP organic matter, it may just reflect the small number of samples examined here. We can exclude that N-bearing organics are more prone to destruction during FIB preparation, and ultramicrotomed IDP sections indeed showed N functionality in some IDPs (25). However, we still see N functionality in the CR organic grains, which have been prepared by FIB as well. IDP organics are in general more aliphatic (25), morphologically more heterogeneous (13), and possibly more pristine, as observed in this work; therefore, the N functionality might be as well different. We could observe that the N–K edge degraded quickly upon electron irradiation even in the aromatic organic matter of the CR chondrites, so it is likely that a different bonding environment of N, i.e., in a more aliphatic component, is more easily destroyed in IDP organics.

We also observe Ca in organic grains 2_24a+b and carbonates in organic grains from GRA 95229. Carbonates and Ca associated with organic amorphous matter have been observed recently, e.g., in Tagish Lake (24) and some other carbonaceous chondrites (32). Usually, this observation is explained by a reaction of an anomalous C–O containing organic precursor with a Ca-enriched fluid leading to the precipitation of carbonates under sufficiently high pH conditions. In the amorphous grains 2_24a+b in this work as well as in some areas of Tagish Lake (24), Ca is associated with an amorphous O-rich organic matter without concomitant crystalline calcites, whereas in our GRA 95229 samples, we indeed observe crystalline calcites in HRTEM images as well as in EEL spectra (Fig. 3 *C* and *D* and Fig. S2). This association is still not well understood, although it is widely observed (e.g., refs. 5 and 24). If these Ca-enriched regions in organic grains (with or without carbonate crystals) are due to the interaction with a Ca-enriched fluid originating within the parent body, the scarcity of such carbonates in the direct vicinity of the grain in NWA 852 is puzzling. However, it is well conceivable that local chemical conditions during aqueous alteration (chemistry and pH) can vary dramatically on a μm scale within meteorite parent bodies (e.g., ref. 48). Within the organic grains of NWA 852, calcite formation was hindered during fluid infiltration, although the intruding Ca-enriched fluids have already reacted with O-rich organic matter to form a homogeneous amorphous grain. There are two other possible explanations for the observed associations of amorphous organic carbon with Ca. First, during FIB preparation and/or SIMS analyses, initially crystalline calcite grains might have been rendered amorphous. However, we consider this to be unlikely because FIB preparation does not amorphize a whole grain several hundreds of nm in diameter. The grain as a whole would then be more heterogeneous. Second, it is possible that Ca or amorphous carbonates were associated with organic matter in the first place, before incorporation into the meteorite parent body, and would then represent a source of indigenous Ca. The association of organic matter with highly soluble Na and Cl has been recently suggested as an indigenous feature of pristine organic matter (28). The essentially anhydrous IDP AK5 grains 8 and 11 also exhibited some Ca in EEL spectra of the organic grains (Fig. S5). Ca has been observed in amorphous metal- and sulfur-rich silicates (5), and recently, Ca has been reported in organic matter from Wild 2 (53). It is therefore conceivable that organic or anhydrous grains in chondritic samples are often intimately mixed with carbonates, because they are genetically connected and form simultaneously. Experiments on carbonate formation in circumstellar environments in the presence of water vapor also indicate that condensation of amorphous carbonates under nonequilibrium conditions can explain the detection of carbonates around evolved stars and protostars (54). On the meteorite parent body, upon local heating due to accretion and radionuclide decay, reactions between the O-rich organic matter and Ca proceeded to form carbonates.

We therefore envision a complex formation scenario for grain 2_24a from NWA 852 that has captured a snapshot of organic modification processes and lends support to organic synthesis models in the solar nebula involving a fluid. A pristine IOM-like organic component has been preserved in the interior of the grain 2_24a, which shows evidence for C–O ketone/aldehyde bonding. This more pristine organic material is also preserved in IDP grains analyzed in this study, where EEL spectra demonstrate evidence for oxygen bonding and no strong indication for aromatic bonding, i.e., a predominance of more labile, more aliphatic components. This pristine component might have contained Ca-bearing molecules initially as we see weak evidence for Ca in IDP organics spectra as well. This O-rich, weakly aromatic organic matter, not necessarily isotopically anomalous, must have been polymerized to the higher-order aromatic matter seen in the rim of this grain, most likely by parent body fluid reactions analogous to the formaldehyde model proposed by Cody et al. (35). By these hydrous reactions, nitrogen enriched in ^{15}N was incorporated into this rim, which was transported from a different locality within the parent body as small soluble ^{15}N-bearing molecules such as ammonia but also still associated with imine/nitrile functional groups. Finally, the material must have been redistributed locally because the N-rich highly aromatic material can also be seen in grain 2_24b next to the rimmed grain, from where a lobe of this material extends down into the meteorite matrix. Nitrogen is apparently prone to these types of redistribution reactions. The strong role of a fluid is also implied by the sharp reaction front between the interior and rim of the grain in STEM-EELS chemical maps (Fig. 1 *C*–*G*). These reactions then have transformed the IOM-like organic precursor into a highly aromatic compound enriched in ^{15}N. Highly aromatic functionality known from some nanoglobules can be observed in this work only in EEL spectra of the CR organic grains, which have been aqueously altered, whereas in the anhydrous IDP organic grains this functionality is less distinct. Our UltraSTEM investigations therefore provide direct evidence that some highly aromatic nanoglobules with high N contents that are ubiquitous in primitive extraterrestrial samples evolve by complex fluid-induced reactions from a more oxygen-rich IOM-like precursor organic material that must not necessarily have been anomalous itself (35). These observations support the view that IDP and CR chondrite organics share a common precursor reservoir, which is preserved in the core of the rimmed grain and the IDP organics. The more processed organic matter as observed in the rim of this grain and the organics from GRA 95229 is then mainly formed by parent body modification processes, which played a vital role in initial organic synthesis (35, 45, 46). An important fraction of complex organic molecules in the early solar system, delivered to the early Earth as part of the most pristine organic inventory, have therefore been synthesized by fluid-induced transformation reactions on asteroids.

Materials and Methods

Isotopically anomalous organic grains have been identified in the Sahara desert CR2 chondrite Northwest Africa (NWA) 852 and the Antarctic CR2 chondrite Graves Nunataks (GRA) 95229 as well as in two CP-IDPs (Table S2). All organic hot spots, isotopically anomalous in D/H, ^{15}N/^{14}N, and/or ^{13}C/^{12}C with respect to the terrestrial values, were detected by standard ion imaging techniques with Cameca NanoSIMS ion probes at the Carnegie Institution of Washington, DC, and the Max Planck Institut für Chemie in Mainz, Germany. Isotopic ratios of detected regions of interest are reported as δ values, which are deviations from the terrestrial standard in ‰ units. Two ^{15}N-enriched organic grains were extracted from each of the CR2 chondrites (Table S2). The IDP AK5 contains numerous ^{15}N- and D-anomalous grains and has a bulk δD of 230 ± 90‰ and a bulk δ^{15}N of 480 ± 30‰ (1σ for all isotopic values). Two ^{15}N-enriched organic grains from this IDP (08 and 11) were chosen for FIB extraction. The second IDP, AK6, contains two ^{15}N-enriched organic grains and one large D-enriched organic grain together with diffuse organic material enriched in D, ^{15}N, and ^{13}C; one ^{15}N-rich and the D-rich organic grain were extracted (09 and 09b). Bulk δD of IDP AK6 is 1570 ± 180‰, and bulk δ^{15}N is

630 ± 110‰. Isotopically anomalous organic grains were relocated in SEMs at the University of Manchester and the MPI in Mainz. FIB preparations were performed on a Zeiss CrossBeam EsB 1540 at the University of Münster and on an FEI Helios NanoLab at the Institute for Functional Materials of the University of Saarbrücken (Germany) applying a special marking protocol (55). We then used a dedicated C_s- (spherical aberration coefficient) corrected Nion UltraSTEM 100 for sample analysis operating at 60 kV in gentle STEM conditions (37). The instrument is equipped with a cold field emission electron source with a nominal energy spread of around 0.3 eV and a quadrupole-octupole C_s-corrector in the condenser system allowing for correction of up to sixfold astigmatism and sub-Ångstrom resolution. The UltraSTEM also has an ultrastable stage, conventional brightfield (BF), and high-angle annular darkfield (HAADF) detectors and a Gatan Enfina EEL spectrometer.

ACKNOWLEDGMENTS. We thank Jutta Zipfel (Senckenberg Museum) for making the NWA 852 thin section available and Cecilia Satterwhite and the Meteorite Working Group for the loan of the GRA 95229 sample. Flavio Soldera and Christoph Pauly (Institute for Functional Materials, University of Saarbrücken) are thanked for preparation of delicate organic grains. We appreciate constructive comments by four anonymous reviewers and the Associate Editor for handling the manuscript. The SuperSTEM Laboratory is the UK National Facility for Aberration-Corrected STEM, supported by the UK Engineering and Physical Sciences Research Council. The work is in part funded by the Deutsche Forschungsgemeinschaft through grants to C.V., J.L., and P.H. in the framework of the SPP 1385. This work is also supported in part by the National Aeronautics and Space Administration (NASA) Astrobiology Institute and NASA Grant NNX10AI63G (to L.R.N.) and Science & Technology Facilities Council grants (to H.B. and N.H.S.).

1. Messenger S (2000) Identification of molecular-cloud material in interplanetary dust particles. *Nature* 404(6781):968–971.
2. Floss C, et al. (2004) Carbon and nitrogen isotopic anomalies in an anhydrous interplanetary dust particle. *Science* 303(5662):1355–1358.
3. Sandford SA, et al. (2006) Organics captured from comet 81P/Wild 2 by the Stardust spacecraft. *Science* 314(5806):1720–1724.
4. Busemann H, et al. (2006) Interstellar chemistry recorded in organic matter from primitive meteorites. *Science* 312(5774):727–730.
5. Busemann H, et al. (2009) Ultra-primitive interplanetary dust particles from the comet 26P/Grigg-Skjellerup dust stream collection. *Earth Planet Sci Lett* 288(1-2):44–57.
6. Aléon J (2010) Multiple origins of nitrogen isotopic anomalies in meteorites and comets. *Astrophys J* 722(2):1342–1351.
7. Bonal L, et al. (2010) Highly ^{15}N-enriched chondritic clasts in the CB/CH-like meteorite Isheyevo. *Geochim Cosmochim Acta* 74(22):6590–6609.
8. Duprat J, et al. (2010) Extreme deuterium excesses in ultracarbonaceous micrometeorites from central Antarctic snow. *Science* 328(5979):742–745.
9. De Gregorio BT, et al. (2010) Isotopic anomalies in organic nanoglobules from Comet 81P/Wild 2: Comparison to Murchison nanoglobules and isotopic anomalies induced in terrestrial organics by electron irradiation. *Geochim Cosmochim Acta* 74(15): 4454–4470.
10. De Gregorio BT, et al. (2011) Correlated microanalysis of cometary organic grains returned by Stardust. *Meteorit Planet Sci* 46(9):1376–1396.
11. De Gregorio BT, et al. (2013) Isotopic and chemical variation of organic nanoglobules in primitive meteorites. *Meteorit Planet Sci* 48(5):904–928.
12. Garvie LAJ, Buseck PR (2004) Nanosized carbon-rich grains in carbonaceous chondrite meteorites. *Earth Planet Sci Lett* 224(3-4):431–439.
13. Matrajt G, Messenger S, Brownlee DE, Joswiak D (2012) Diverse forms of primordial organic matter identified in interplanetary dust particles. *Meteorit Planet Sci* 47(4): 525–549.
14. Hashiguchi M, Kobayashi S, Yurimoto H (2013) In situ observation of D-rich carbonaceous globules embedded in NWA 801 CR2 chondrite. *Geochim Cosmochim Acta* 122:306–323.
15. Nakamura-Messenger K, Messenger S, Keller LP, Clemett SJ, Zolensky ME (2006) Organic globules in the Tagish Lake meteorite: Remnants of the protosolar disk. *Science* 314(5804):1439–1442.
16. Garvie LAJ, Buseck PR (2006) Carbonaceous materials in the acid residue from the Orgueil carbonaceous chondrite meteorite. *Meteorit Planet Sci* 41(4):633–642.
17. Terzieva R, Herbst E (2000) The possibility of nitrogen isotopic fractionation in interstellar clouds. *Mon Not R Astron Soc* 317(3):563–568.
18. Rodgers SD, Charnley SB (2008) Nitrogen isotopic fractionation of interstellar nitriles. *Astrophys J* 689(2):1448–1455.
19. Lyons JR (2009) N_2 self-shielding in the solar nebula. *Meteorit Planet Sci* 44: A5437 (abstr).
20. Lyons JR (2012) Isotope signatures in organics due to CO and N2 self-shielding. *Lun Planet Sci Conf* 43: abstr.# 2858.
21. Muskatel BH, Remacle F, Thiemens MH, Levine RD (2011) On the strong and selective isotope effect in the UV excitation of N2 with implications toward the nebula and Martian atmosphere. *Proc Natl Acad Sci USA* 108(15):6020–6025.
22. Chakraborty S, et al. (2014) Are organic macromolecules in meteorites formed within the solar system? *Lunar Planet Sci Conf* 45:2452 (abstr 2452).
23. Hoppe P, Cohen S, Meibom A (2013) NanoSIMS: Technical aspects and applications in cosmochemistry and biological geochemistry. *Geostand Geoanal Res* 37(2):111–154.
24. Zega TJ, et al. (2010) Mineral associations and character of isotopically anomalous organic material in the Tagish Lake carbonaceous chondrite. *Geochim Cosmochim Acta* 74(20):5966–5983.
25. Keller LP, et al. (2004) The nature of molecular cloud material in interplanetary dust. *Geochim Cosmochim Acta* 68(11):2577–2589.
26. Busemann H, et al. (2007) Secondary ion mass spectrometry and X-ray absorption near-edge structure spectroscopy of isotopically anomalous organic matter from CR1 chondrite GRO95577. *Lunar Planet Sci Conf* 38:1884 (abstr 1884).
27. Le Guillou C, Bernard S, Brearley AJ, Remusat L (2014) Evolution of organic matter in Orgueil, Murchison and Renazzo during parent body aqueous alteration: In situ investigations. *Geochim Cosmochim Acta* 131:368–392.
28. Le Guillou C, Brearley AJ (2014) Relationships between organics, water and early stages of aqueous alteration in the pristine CR3.0 chondrite MET 00426. *Geochim Cosmochim Acta* 131:344–367.
29. Floss C, Le Guillou C, Brearley AJ (2014) Coordinated NanoSIMS and FIB-TEM analyses of organic matter and associated matrix material in CR3 chondrites. *Geochim Cosmochim Acta* 139:1–25.
30. Cody GD, et al. (2008) Quantitative organic and light-element analysis of comet 81P/Wild 2 particles using C-, N-, and O-μ-XANES. *Meteorit Planet Sci* 43(1-2):353–365.
31. Le Guillou C, et al. (2012) High resolution TEM of chondritic carbonaceous matter: Metamorphic evolution and heterogeneity. *Meteorit Planet Sci* 47(3):345–362.
32. Le Guillou C, Remusat L, Bernard S, Brearley AJ (2011) Redistribution and evolution of organics during aqueous alteration: NanoSIMS - STXM - TEM analyses of FIB sections from Renazzo, Murchison and Orgueil. *Lunar Planet Sci Conf* 42:1996 (abstr).
33. Derenne S, Robert F (2010) Model of molecular structure of the insoluble organic matter isolated from Murchison meteorite. *Meteorit Planet Sci* 45(9):1461–1475.
34. Saito M, Kimura Y (2009) Origin of organic globules in meteorites: Laboratory simulation using aromatic hydrocarbons. *Astrophys J* 703(2):L147–L151.
35. Cody GD, et al. (2011) Establishing a molecular relationship between chondritic and cometary organic solids. *Proc Natl Acad Sci USA* 108(48):19171–19176.
36. Kebukawa Y, Kilcoyne ALD, Cody GD (2013) Exploring the potential formation of organic solids in chondrites and comets through polymerization of interstellar formaldehyde. *Astrophys J* 771(1):19.
37. Krivanek OL, et al. (2010) Gentle STEM: ADF imaging and EELS at low primary energies. *Ultramicroscopy* 110(8):935–945.
38. Zobelli A, Gloter A, Ewels CP, Seifert G, Colliex C (2007) Electron knock-on cross section of carbon and boron nitride nanotubes. *Phys Rev B* 75:245402.
39. Buban JP, Ramasse Q, Gipson B, Browning ND, Stahlberg H (2010) High-resolution low-dose scanning transmission electron microscopy. *J Electron Microsc (Tokyo)* 59(2): 103–112.
40. Heymann K, Lehmann J, Solomon D, Schmidt MWI, Regier T (2011) C 1s K-edge near edge X-ray absorption fine structure (NEXAFS) spectroscopy for characterizing functional group chemistry of black carbon. *Org Geochem* 42(9):1055–1064.
41. Cody GD, et al. (2008) Organic thermometry for chondritic parent bodies. *Earth Planet Sci Lett* 272(1-2):446–455.
42. Flynn GJ, Wirick S, Keller LP, Jacobsen C, Sandford SA (2010) Organic coatings on individual grains in CP IDPs: Implications for the formation mechanism of pre-biotic organic matter and for grain sticking in the early solar system. *Lunar Planet Sci Conf* 41:1079 (abstr).
43. Herd CDK, et al. (2011) Origin and evolution of prebiotic organic matter as inferred from the Tagish Lake meteorite. *Science* 332(6035):1304–1307.
44. Alexander CMOD, et al. (2014) Elemental, isotopic, and structural changes in Tagish Lake insoluble organic matter produced by parent body processes. *Meteorit Planet Sci* 49(4):503–525.
45. Alexander CMOD, Fogel M, Yabuta H, Cody GD (2007) The origin and evolution of chondrites recorded in the elemental and isotopic compositions of their macromolecular organic matter. *Geochim Cosmochim Acta* 71(17):4380–4403.
46. Alexander CMOD, et al. (2010) Deuterium enrichments in chondritic macromolecular material—Implications for the origin and evolution of organics, water and asteroids. *Geochim Cosmochim Acta* 74(15):4417–4437.
47. Ciesla FJ, Sandford SA (2012) Organic synthesis via irradiation and warming of ice grains in the solar nebula. *Science* 336(6080):452–454.
48. Brearley AJ (2006) The action of water. *Meteorites and the Early Solar System II* (Univ of Ariz Press, Tucson), pp 587–624.
49. Apen E, Hitchcock AP, Gland JL (1993) Experimental studies of the Core Excitation of Imidazole, 4,5-Dicyanoimidazole, and s-Triazine. *J Phys Chem* 97(26):6859–6866.
50. Hily-Blant P, Bonal L, Faure A, Quirico E (2013) The ^{15}N-enrichment in dark clouds and Solar System objects. *Icarus* 223(1):582–590.
51. Peeters Z, Changela H, Stroud RM, Alexander CMOD, Nittler LR (2012) Organic carbon inclusions in CR2 chondrite Graves Nunataks 95229. *Meteorit Planet Sci* 47:A312.
52. Pizzarello S, Williams LB (2012) Ammonia in the early Solar System: An account from carbonaceous chondrites. *Astrophys J* 749(2):161–166.
53. De Gregorio BT, Stroud RM, Nittler LR (2014) Extreme aliphatic and aromatic organic matter preserved in comet 81P/Wild 2. *Lunar Planet Sci Conf* 45:2759 (abstr).
54. Toppani A, et al. (2005) A 'dry' condensation origin for circumstellar carbonates. *Nature* 437(7062):1121–1124.
55. Holzapfel C, Soldera F, Vollmer C, Hoppe P, Mücklich F (2009) TEM foil preparation of sub-um sized grains by the focused ion beam technique. *J Electron Microsc (Tokyo)* 235(1):59–66.